Defense Threat Reduction Agency
8725 John J. Kingman Road, MS-6201
Fort Belvoir, VA 22060-6201

DTRA-TR-13-52

TECHNICAL REPORT

Biocidal Energetic Materials for the Destruction of Spore Forming Bacteria

July 2015

HDTRA1-10-1-0108

Emily M. Hunt

Prepared by:
West Texas A&M University
P.O. Box 60767
Canyon, TX 79016

DESTRUCTION NOTICE:

Destroy this report when it is no longer needed.
Do not return to sender.

PLEASE NOTIFY THE DEFENSE THREAT REDUCTION AGENCY, ATTN: DTRIAC/ J9STT, 8725 JOHN J. KINGMAN ROAD, MS-6201, FT BELVOIR, VA 22060-6201, IF YOUR ADDRESS IS INCORRECT, IF YOU WISH THAT IT BE DELETED FROM THE DISTRIBUTION LIST, OR IF THE ADDRESSEE IS NO LONGER EMPLOYED BY YOUR ORGANIZATION.

REPORT DOCUMENTATION PAGE

Form Approved
OMB No. 0704-0188

1. REPORT DATE *(DD-MM-YYYY)*	**2. REPORT TYPE**	**3. DATES COVERED** *(From - To)*
00-07-2015	Technical	N/A

4. TITLE AND SUBTITLE

Biocidal Energetic Materials for the Destruction of Spore Forming Bacteria

5a. CONTRACT NUMBER

HDTRA1-10-1-0108

5b. GRANT NUMBER

5c. PROGRAM ELEMENT NUMBER

6. AUTHOR(S)

Emily M. Hunt, Ph.D.

5d. PROJECT NUMBER

5e. TASK NUMBER

5f. WORK UNIT NUMBER

7. PERFORMING ORGANIZATION NAME(S) AND ADDRESS(ES)

West Texas A&M University
Box 60767
Canyon, TX 79016

8. PERFORMING ORGANIZATION REPORT NUMBER

9. SPONSORING / MONITORING AGENCY NAME(S) AND ADDRESS(ES)

Defense Threat Reduction Agency
8725 John J. Kingman Road STOP 6201
Fort Belvoir, VA 22060

10. SPONSOR/MONITOR'S ACRONYM(S)

DTRA

11. SPONSOR/MONITOR'S REPORT NUMBER(S)

DTRA-TR-13-52

12. DISTRIBUTION / AVAILABILITY STATEMENT

Distribution Statement A. Approved for public release; distribution is unlimited.

13. SUPPLEMENTARY NOTES

14. ABSTRACT

The objectives of this project are to fundamentally understand the interaction between spore forming bacteria and thermite reactions and products and to exploit energetic material reactions with biocidal properties to destroy bacteria and investigate how the properties of individual nano-scale particles influence their macroscopic combustion behaviors and mechanisms of interactions with spore forming bacteria. These objectives will be addressed through examining the response of spores exposed to gas generating thermites that include iodine or other halogen species that demonstrate the potential to neutralize bacteria. This investigation will characterize the gas phase chemical species responsible for bacterium neutralization as well as examine the thermal and physical effects, such as exposure time, on spore destruction. Reaction kinetics of the candidate thermites will also be studied to elucidate the mechanisms of destruction.

15. SUBJECT TERMS

Bacteria Spore Gas Antibacterial Thermal

16. SECURITY CLASSIFICATION OF:			**17. LIMITATION OF ABSTRACT**	**18. NUMBER OF PAGES**	**19a. NAME OF RESPONSIBLE PERSON**
a. REPORT	**b. ABSTRACT**	**c. THIS PAGE**	SAR	47	Suhithi Peiris
Unclassified	Unclassified	Unclassified			**19b. TELEPHONE NUMBER** *(include area code)* 703-767-4732

CONVERSION TABLE

Conversion Factors for U.S. Customary to metric (SI) units of measurement.

MULTIPLY →	BY →	TO GET
TO GET ←	BY ←	DIVIDE
angstrom	1.000 000 x E -10	meters (m)
atmosphere (normal)	1.013 25 x E +2	kilo pascal (kPa)
bar	1.000 000 x E +2	kilo pascal (kPa)
barn	1.000 000 x E -28	meter^2 (m^2)
British thermal unit (thermochemical)	1.054 350 x E +3	joule (J)
calorie (thermochemical)	4.184 000	joule (J)
cal (thermochemical/cm^2)	4.184 000 x E -2	mega joule/m^2 (MJ/m^2)
curie	3.700 000 x E +1	*giga bacquerel (GBq)
degree (angle)	1.745 329 x E -2	radian (rad)
degree Fahrenheit	$t_k = (t^of + 459.67)/1.8$	degree kelvin (K)
electron volt	1.602 19 x E -19	joule (J)
erg	1.000 000 x E -7	joule (J)
erg/second	1.000 000 x E -7	watt (W)
foot	3.048 000 x E -1	meter (m)
foot-pound-force	1.355 818	joule (J)
gallon (U.S. liquid)	3.785 412 x E -3	meter^3 (m^3)
inch	2.540 000 x E -2	meter (m)
jerk	1.000 000 x E +9	joule (J)
joule/kilogram (J/kg) radiation dose absorbed	1.000 000	Gray (Gy)
kilotons	4.183	terajoules
kip (1000 lbf)	4.448 222 x E +3	newton (N)
kip/inch^2 (ksi)	6.894 757 x E +3	kilo pascal (kPa)
ktap	1.000 000 x E +2	newton-second/m^2 ($N-s/m^2$)
micron	1.000 000 x E -6	meter (m)
mil	2.540 000 x E -5	meter (m)
mile (international)	1.609 344 x E +3	meter (m)
ounce	2.834 952 x E -2	kilogram (kg)
pound-force (lbs avoirdupois)	4.448 222	newton (N)
pound-force inch	1.129 848 x E -1	newton-meter (N-m)
pound-force/inch	1.751 268 x E +2	newton/meter (N/m)
pound-force/foot^2	4.788 026 x E -2	kilo pascal (kPa)
pound-force/inch^2 (psi)	6.894 757	kilo pascal (kPa)
pound-mass (lbm avoirdupois)	4.535 924 x E -1	kilogram (kg)
pound-mass-foot^2 (moment of inertia)	4.214 011 x E -2	kilogram-meter^2 ($kg-m^2$)
pound-mass/foot^3	1.601 846 x E +1	kilogram-meter^3 (kg/m^3)
rad (radiation dose absorbed)	1.000 000 x E -2	**Gray (Gy)
roentgen	2.579 760 x E -4	coulomb/kilogram (C/kg)
shake	1.000 000 x E -8	second (s)
slug	1.459 390 x E +1	kilogram (kg)
torr (mm Hg, 0^0 C)	1.333 22 x E -1	kilo pascal (kPa)

*The bacquerel (Bq) is the SI unit of radioactivity; 1 Bq = 1 event/s.

**The Gray (GY) is the SI unit of absorbed radiation.

Objectives:

The objectives of this project are to fundamentally understand the interaction between spore forming bacteria and thermite reactions and products and to exploit energetic material reactions with biocidal properties to destroy bacteria and investigate how the properties of individual nano-scale particles influence their macroscopic combustion behaviors and mechanisms of interactions with spore forming bacteria. These objectives will be addressed through examining the response of spores exposed to gas generating thermites that include iodine or other halogen species that demonstrate the potential to neutralize bacteria. This investigation will characterize the gas phase chemical species responsible for bacterium neutralization as well as examine the thermal and physical effects, such as exposure time, on spore destruction. Reaction kinetics of the candidate thermites will also be studied to elucidate the mechanisms of destruction. This project introduces two distinct approaches of:

(1) creating a highly porous, solid products with naturally antibacterial and biocidal properties using combustion synthesis of mildly energetic reactants; and,

(2) engineering an aerosolized spray of biocidal gases using unique a deflagration synthesis approach.

Accomplishments for all years:

Major Activity 1: Creating highly porous antibacterial solid materials through combustion synthesis

Specific Objectives:

a. Characterize how the balance of reactants influences the combustion and bactericidal behaviors of the product foam.

b. Evaluate the impact of heating rate on the combustion of the foam product.

c. Investigate the Biocidal Properties of the Foam Product

This study examines a method to create highly porous, antibacterial solid materials (or foams) through combustion synthesis. By combining nano-scale Silver Oxide (Ag_2O) or TiO_2 particles with Aluminum (Al) nano-scale particles, the reaction produces a self-propagating heat wave that will synthesize metallic foams made of pores only nanometers wide that inherently exhibits antibacterial properties. The extraordinarily high surface areas these foams possess serve as an excellent platform for the neutralization of bacteria. These newly synthesized alloys present a novel approach to bacterial neutralization.

Experiments are performed to demonstrate the bacterial growth kinetics on synthesized foams. Bacillus Subtilis is a spore-forming bacterium like anthrax but benign and is used for this study. The first experimental results are obtained for mixtures composed of Al/Ag_2O and Al/TiO_2. Experiments are also conducted on micron-scale Al/Ag_2O to examine the effect of the particle size. The nanometer aluminum particles (nmAl) are obtained by NovaCentrix with an average particle diameter of 50 nm passivated with an average alumina shell thickness of 2 nm and are spherical in shape. The 10 micrometer Al (micron Al) particles have an estimated 3 nm thick oxide shell and are also spherical. All other metal oxide particles also exhibit spherical morphology. The Ag_2O was purchased from Sigma-Aldrich in two different sizes and has an average particle diameter of 30 microns and 100 nm. Particle size, Al shell thickness and morphology information were provided by the suppliers. Each mixture was prepared for a stoichiometric equivalence ratio of 1.0. Each sample contains 100 mg of reactant mixture and density can be varied from 5% (loose powder) to cold pressed at a theoretical maximum density of 70%.

Self-propagating high-temperature synthesis (SHS) is used to create the metallic foams and the experimental set-up. A metallic foam is created when a mildly energetic composite includes a modest amount of gasifying agent (GA). During a reaction the GA generates nucleation sites that promote the formation of bubbles. As the reaction wave passes, the gas pockets within the bubbles escape leaving a porous structure. In previous combustion synthesis studies, a GA may be added as a separate reactant usually in the form of a powder or granular material. In this study, the metal oxide nanoparticles act as the GA in each mixture. Most previous work pertaining to the synthesis of porous materials using combustion synthesis was limited to micron-scale reactant particles.

The product foams are then placed on an agar plate and 50 μL of Bacillis Subtilis is applied directly on and around the material. The metallic foams are placed in an incubator for 24 hours at 37°C and then removed and checked for bacterial growth. The samples are then placed back into the incubator for another 24 hours and the results are discussed below.

Experiments show no bacterial growth after 24 hours on the nano Ag_2O or nano TiO_2, but does show colony forming unit (CFU) growth areas on the micron Ag_2O nanofoam. After 48 hours, there are significant CFUs on all of the foams, except for the nano $AlAg_2O$ which shows no sign of any bacteria. A Rigaku Ultima III X-ray diffractometer (40 kV, 44 mA, Cu Kα radiation) was employed for X-ray powder diffraction measurements (XRD).The specimens were scanned from 20.0 to 80.0 degrees in 0.15 second intervals at the resolution of 0.03 degrees and the results give insight into the actual product composition of the metallic nanofoams. The nano Al+Ag2O show significant percentages of Ag in the products while the micron $Al+Ag_2O$ samples show high amounts of $Ag_{0.55}Al_{0.35}$. Of the metal ions, silver exhibits the highest toxicity for microorganisms and the least toxicity to animal cells. The antimicrobial spectrum of silver is extensive, including gram-negative aenterobacteria and gram-positive cocci. When silver particles approach nano-scale dimensions they exhibit increased chemical activity due to their large surface to volume

ratios and crystallographic surface structure. The bactericidal properties of the nanoparticles are size dependent, and initial studies on nanocrystalline silver confirm that their material structure is unique leading to its effectiveness as an antifungal and antibacterial agent.

Key Outcomes:

1. Combustion synthesis can be used to create materials that have antibacterial properties.
2. Bacteria growth kinetics are a function of reactant particle size.
3. Nanoscale reactants are more effective in neutralizing bacteria.
4. TiO2 particles can delay, but not prevent bacterial growth, and;
5. antibacterial metallic nanofoams can be easily created as a structural material or a metallic coating through combustion synthesis and have far-reaching applications.

Please see the attached article for more detailed information.

Major Activity 2: Generating biocidal gases through deflagration synthesis

Specific Objectives:

a. Explore the coupling of thermal and chemical effects.

b. Examine effect of environmental conditions on bacterial efficacy.

c. Investigate the kinetics of halogen containing oxides.

Significant Results:

The objective of this study is to understand the components preceeding and enabling the deactivation of *Bacillus thuringiensis* spores, with variable temperature and iodine gas treatements. This is accomplished by experiments that isolate and focus on the effects of temperature, iodine gas and the combination of the two parameters, allowing for quantifiable comparisons between treatments and analysis of the efficacy of deactivation.

It is critical in the destruction of spore forming bacteria to fundamentally examine the components enabling deactivation of *Bacillus thuringiensis*. The deactivation is attributed to the thermal effect of the heat on the spore and the associated chemical effect of halogen gas (i.e., produced from thermite combustion). Results show heat transfer in the spore enhances the effectiveness of the halogen gasses in the deactivation process and that elevated temperatures increase spore permeability, facilitating gas penetration and accelerating spore deactivation. These results provide molecular-level insights into the components underpinning biological processes leading to spore neutralization.

The results of this study lay the foundation upon which the efficiency of thermite bacterial deactivation may be improved. Analyses of dwell times reveal parameters directly affecting

bacterial deactivation when utilizing both heat and biocidal iodine gas. This knowledge being previously related to biocidal solutions only and not gasses. Yet, gas generation and dispersion may be an important method for improving spatial neutralization of biocidal agents, especially those related to mass bacterial spore destruction.

Bacillus Thuringiensis Neutralization Using a Thermo-Chemical Combination

Numerous papers and a great number of researches have observed the effectiveness of Iodine and temperature to neutralize different bacillus types. Iodine has been shown to be very effective yet relatively slow in its neutralization of bacterial spores. A sizeable reduction in dwell time would render Iodine a major tool in the area of bacterial neutralization. Bacteria exposed solely to temperature have been observed to reach a point of inactivation, yet these required really high temperatures and dwell times. Having observed the individual abilities of these two mediums, experiments were setup to observe and study the behavior and effectiveness in neutralization of combining the Iodine and temperature.

The setup consisted of a biocidal exposure chamber in which dried Bacillus thuringiensis was exposed to iodine gas and temperature. The biocidal exposure chamber was made of glass allow for quick even distribution of the heat. Iodine crystals where used instead of combusting an Aluminum Iodine Pentoxide mix. This allowed the focus to be primarily on the effect of the generated gas, temperature and the exposure times.

A wide range of temperatures were tested with a constant amount of iodine. The observed range of temperatures was from 700C-1300C in increments of 100C. The observed exposure time were 15, 30 and 45 minutes respectively. Tests were performed observing both the effects of just the temperature and also the combination of temperature and iodine gas. This would allow for observation of the balance of each agent in the neutralization process.

Initial tests in the 700C-1000C range, showed no effects to the combination of the thermal and chemical attack. Minor results were observed at a 1000C for the maximum exposure time of 45 minutes. Effective results from the combination of iodine and temperature were observed in the 1100C-1200C range. In this range effective neutralization was observed at the minimal dwell time of 15 minutes. From the observations it was deduced that the neutralization in this range was due more to the presence of the iodine, than to the temperature. This can be confirmed by observing the temperature only tests which show that temperature alone shows no effects until it is above the 1200C point. Therefore there appears to be an optimal range at which the combination of the thermal and chemical aspects prove to be most effective, at reduced temperatures. A continued increase in temperature does show effective neutralization at the minimal allocated dwell time.

The ability to effectively decrease the dwell time of iodine has to this point not been observed. This study has shown that it is indeed a possibility and that an optimal range of temperature

exists that facilitates the neutralizing capabilities of iodine. These observations have led to the initiating of 2 new studies. Firstly a thorough investigation of the observed optimal temperature range to see how small a dwell time can be achieved. Secondly a study into the mechanisms that renders a spore more quickly susceptible to neutralization due to the combination of a thermal and chemical effect.

Humidity's effect on iodine neutralization of Bacillus Thuringiensis spores

Iodine's antibacterial properties are well known; because of this, reactive materials that release iodine gas have been studied for their ability to neutralize bacteria. These studies have shown iodine producing reactive materials are effective against spore forming bacteria, but are sensitive to the relative humidity in the testing environment. Results from tests run in relative high humidity environments show a decreased ability of iodine to effectively neutralize bacteria during a one hour exposure. This could be caused by iodine's ability to be dissolved into water. This reduces the concentration of iodine in the environment reducing the ability to neutralize bacteria. Characterizing these reactions' sensitivity to humidity is important to determine their abilities as biocidal agents.

These tests were conducted using a sealed blast chamber with a drying train consisting of 2 blower motors and a silica desiccant drying chamber. These tests were conducted at 35 percent (atmospheric) and at 24 percent humidity using two different reactive materials, $Al + I_2O_5$ and $Al + Ca(IO_3)_2$. Two tests for each combination of reactive material and humidity were conducted with 4 samples of dried Bacillus Thuringiesis per test. Each sample consisted of 0.1mL of a 10^6 spores per 0.1mL BT spore suspension; which were then dried for 24 hours at 37oC. For each test 250 mg of RM was placed in the center of the BRC and the sample vials were placed 12 cm up in the walls of the BRC.

The results of the 35 percent humidity tests showed neither reactive material significantly decreased spore growth when compared to the control plates. During these test iodine pools formed in BRC after the one hour exposure time; showing that the Iodine was combining with the moisture in the air. The 24 percent humidity test showed strong evidence of a reduction in spore growth when compared to the non-exposed control plates. No evidence of iodine pooling was evident after the one hour exposure time.

These preliminary results give evidence that the ability of iodine to neutralize bacteria is sensitive to the humidity in the surrounding environment. Iodine's hygroscopic nature could explain this sensitivity, the iodine that is released by the reaction combines with the moisture in the environment to produce ionic acid.

Kinetics of Nanoenergetics with Halogen Containing Oxides

Because iodine has been shown to be effective in neutralizing spore form bacteria, reactions that have gaseous iodine as a product need to be characterized in order to effectively utilize their products to battle these bacteria. In order to produce halogen gases, compounds containing both a halogen gas and oxygen were selected. Due to the electronegativity of chlorine (3.16), iodine (2.66) and oxygen (3.44), reaction containing either of these halogens and oxygen have the potential for the aluminum to react with oxygen leaving the halogen gas as a free gas product. The four compounds mixed with aluminum were I_2O_5, $Ca(IO_3)_2$, $AgIO_3$, $KClO_4$.

Both thermal equilibrium and non-equilibrium test were performed and the results compared to REAL code modeling software in order to gauge the energy output and relative efficiencies of each reaction at each reaction rate. A Neztsch STA 409 differential scanning calorimeter and thermogravimetric analyzer (DSC/TGA) was used for the thermal equilibrium test. An ~8mg sample was loaded into a platinum crucible with an alumina liner and placed on a sample carrier inside an oven and heated at 10K/min until the reaction was complete. The crucible lid was vented in order to prevent pressurization within the device. The reacting crucible was compared to an empty reference crucible in order to obtain the net energetic and mass changes. Also, the sample carrier is mounted on a microscale allowing for mass change measurements that relay information as to the gas production nature of the reactants and products at the various temperatures. The area under the DSC curve was used to obtain the net exothermic behavior of each given reaction.

For the non-equilibrium tests, a Parr model 1341 bomb calorimeter was used with a model 1108 oxygen combustion bomb chamber. Using REAL code values for theoretical heats of combustion based on the heat of formation for the reactants and products, powder massed were determined in order to obtain a 0.5 to 1K elevation of a 2kg water bath above the calibrated energy inputs of a stirrer and other environmental factors. Using a 60% value between the lines extrapolated before and after the reaction on a temperature vs time plot, a dT value was obtained in order to find the energy associated with heating the steel bomb chamber and water.

The results show that 10Al+3I2O5 is the most energetic formulation. In the thermo-equilibrium environment, this reaction also had the largest mass loss at 85%. The mass loss began before the temperature was high enough to activate the aluminum causing some reactant loss, which partially accounts for the reduced exothermic behavior in the DSC experiments when compared to the bomb calorimeter. The high energy and gas production is consistent with a reaction that produces a iodine in a violent and percussive manner. A much less violent reaction with a large mass loss of 73% is the reaction $4Al+Ca(IO_3)_2$. The reaction is 28% less energetic than $10Al+3I_2O_5$ in the bomb calorimeter. The lower energetic nature and gas production implies that the reaction would produce iodine gas in a more controlled, less destructive nature than the $10Al+3I_2O_5$ reaction with $2Al+AgIO_3$ falling in between.

In an effort to attempt to obtain chlorine gas in a reaction, $KClO_4$ was used, but the resulting products have no gas production since the potassium and chlorine remained bonded after the combustion.

The most recent results suggest a synergistic behavior between the iodine gas and temperature in the deactivation of *Bacillus thuringiensis*. Due to the modes of deactivation this synergistic behavior may be beneficial in the reduction of dwell times. In regard to thermite reactions and their thermal propagation gradient, this knowledge would prove useful in potentially improving deactivation efficiency. The results suggest a thermite reaction with increased spatial temperature distribution and slow burning characteristics could potentially show sizable improvements as a spore neutralization medium.

Composite energetic materials that include biocidal agents have recently spurred interest for their potential to deactivate spore forming bacteria. We have examined the feasibility of this approach using bacterial spores that include bacillus thuringiensis and bacillus anthracis exposed to energetic formulations that include iodine, such as aluminum and iodine pentoxide ($Al\text{-}I_2O_5$). These fundamental studies resulted in an understanding that a balance of two primary reaction parameters needs to be coupled in order to reduce dwell times: temperature and the production of iodine gas. However, those studies examined spore neutralization on the order of minutes while the current impetus is to deactivate spore forming bacteria within milliseconds. Towards this end, the results from previous studies have been extrapolated to the millisecond time regime in an effort to identify the potential reaction conditions that will ensure deactivation. The Pearson product-moment correlation confirmed linear dependence of the data prior to the extrapolation and results show that the coupled thermal-biocidal gas mechanism will require elevated temperatures of 360^oC and allow for 80% deactivation in tens of milliseconds while thermal conditions alone would require nearly 1000^oC for the same deactivation.

It should be noted that the energetic formulations such as $Al\text{-}I_2O_5$, AlI_x, and Al-AgIO all produce locally isolated elevated temperatures, localized near the source. The spatial distribution of temperature from any of these composite energetic materials has been documented to exponentially decrease with distance from the reaction. Using these formulations for these biocidal applications would require additives to the formulation that would increase the spatial distribution of temperature or perhaps influence the permeability of the spore such that biocidal gas transport can be accelerated. Other contributing factors not examined yet include pressure waves from detonating mixtures. In unconfined settings, these candidate formulations deflagrate such that pressure influences are negligible. However, confining these mixtures or adding explosives may facilitate compression waves that may also contribute to deactivation.

Key Outcomes:

1. Reduction of dwell time is feasible and can be achieved with an optimum combination of temperature and iodine gas.
2. Initial study indicates that humidity plays a role in the ability of iodine-based oxidizers to neutralize BT spores. Lowering the moisture in the air allows the larger amount of iodine to remain in its gas phase longer.
3. Ca(IO3)2 is a viable alternative to I_2O_5 as an iodine-based biocidal oxidizer.
4. A new theory is presented for cell deactivation based on the permeability of the cell structure.
5. The coupled thermal-biocidal gas mechanism will require elevated temperatures of 360^{o}C and allow for 80% deactivation in tens of milliseconds while thermal conditions alone would require nearly 1000^{o}C for the same deactivation.

Please see the attached articles for more information on this topic.

Personnel Supported:

	Personnel								
Award #:[1]	**PIs/Co-PIs [2]**	**Post-Doctoral Fellows [2,3]**		**Graduate Students [2,3]**		**Undergraduate Students [2,3]**		**Research Technicians [2]**	**PI's Hirsch Index [4]**
		U.S. + non-U.S.	**U.S.**	**U.S. + non-U.S.**	**U.S.**	**U.S. + non-U.S.**	**U.S.**		
HDTRA-1-08-10-BRCWMD	2	0	0	5	4	9	9	0	14

[1] Enter Award #, starts with "HDTRA"

[2] Enter number of U.S. + non-U.S. personnel working on this award

[3] Enter number of U.S. personnel working on this award

[4] Enter PI's Hirsch Index

Five graduate students and nine undergraduates have been trained on state of the art diagnostic equipment to perform purposeful experiments and analyze results. Diagnostic training included differential scanning calorimetry, thermal gravimetric analysis, quadrupol mass spectrometry, high speed imaging systems, advanced infrared diagnostics for temperature measurements and laser spectroscopy systems. In addition, students have had safety training relating to this, handling of energetic materials and chemical lab safety as well as detailed protocols for the safe handling and use of bacteria samples.

Publications:

Publications								
Year	Publications (Peer-Reviewed Journals) [5]		Publications (Proceedings) [6]	Publications (Books) [7]	Publications (Theses) [8]		Publications (Other) [9]	Invention Disclosures [10]
	Published	Submitted, in review, accepted, or in press			Ph.D.	Masters		
2011 (after 9/1/11)	0	0	2	0	0	1	1	1
2012	0	4	2	0	0	1	1	1

[5] Enter total number of peer-reviewed publications for this award (includes only published (print and online)) for this reporting period

[5] Include additional peer reviewed pubs that are "submitted", "in review", "accepted", or "in press"

[6] Enter number of non-peer reviewed conference proceedings articles for this award for this reporting period

[7] Enter number of published books or chapter of books for this reporting period

[8] Enter number of Ph.D. dissertations and Masters Theses for this reporting period

[9] Enter number of other publications for this reporting period

[10] Enter number of invention disclosures

Peer Reviewed Publications:

1. Nanostructured Antibacterial Metallic Alloys, *MRS Communications*, accepted with revisions and in press 2012.
2. Permeability acclimatization responsible for dwell time reductions in spore deactivation, *Journal of Applied Molecular Biology*, submitted May 2012.
3. Engineered Antibacterial Materials, *Journal of Biology and Nanotechnology*, submitted July 2012.
4. Spore Deactivation Conditions Necessary for Millisecond Dwell Times, *Acta Biomaterialia*, submitted July 2012.
5. Designing Dandelions, Texas Tech University Press, in press 2013. This is a children's book that was developed to teach children about the concepts of energy generation and the engineering design process.

Peer-Reviewed Conference Proceedings:

1. Mulamba, O, Pantoya ML, and Hunt, EM, Thermal Influences on the Neutralization of Spore Forming Bacteria, ASME Heat Transfer Conference, Puerto Rico (2012).

Honors/Awards:

1. Distinguished Faculty Award, West Texas A&M University Alumni Association, May 2012.
2. Amarillo Women's Network Career Achievement Award, September 2011.
3. Intellectual Contribution Award, West Texas A&M University, 2011.

Courses taught: Combustion, MENG 4392, undergraduate mechanical engineering class teaching the basics of combustion with special topics section on CWMDs. Taught three times with 50+ students each time.

Synthesis of Antibacterial Metallic NanoFoams

Emily M. Hunt, Ph.D., Department of Engineering and Computer Science, West Texas A&M University, Canyon, TX, 79016

Michelle L. Pantoya, Ph.D., Department of Mechanical Engineering, Texas Tech University, Lubbock, TX 79409

Abstract

Antibacterial metallic nanomaterials are created as a structural material or a metallic coating through combustion synthesis and have far-reaching applications in the food service and medical industry. This study examines a method to create highly porous, solid materials (or foams) through combustion synthesis. By combining nano-scale Silver Oxide (Ag_2O) or Titanium Dioxide (TiO_2) particles with nano-scale Aluminum (Al) particles, the reaction can produce a self-propagating heat wave that will synthesize metallic foams made of pores only nanometers wide that inherently exhibit antibacterial properties. The extraordinarily high surface areas these foams possess serve as an excellent platform for the neutralization of bacteria.

Bacterial contamination in hospitals, food industries, and public environments create a major public health issue. Despite considerable research and development efforts, the problem of contaminations related to biomedical devices and food preparation persists. Traditional cleaning methods, such as aerosolized disinfectant sprays or wipes have a limited effectiveness. There is a strong need to mitigate bacterial colonization by engendering materials with properties that include surface chemistry [1-3] and surface roughness [4-6] which are unfavorable for bacterial attachment and growth.

Silver has been used for years in many bactericidal applications because of its strong toxicity to a wide range of micro-organisms [1-8]. Research has shown that the bactericidal properties of silver are size dependent, and only nanoparticles present a direct interaction with the bacteria [3]. Titanium dioxide (TiO_2) has also become a popular agent for bacterial neutralization. Several commercial products have been developed that incorporate nanoparticles of TiO_2 for antibacterial applications [9].

This study examines a method to create highly porous, antibacterial solid materials (or foams) through combustion synthesis. By combining nano-scale Silver Oxide (Ag_2O) or nano-scaleTiO_2 particles with Aluminum (Al) nano-scale particles, the reaction can produce a self-propagating heat wave that will synthesize metallic foams made of pores only nanometers wide that inherently exhibit antibacterial properties. The extraordinarily high surface areas these foams possess serve as an excellent platform for the neutralization of bacteria. These newly synthesized alloys present a novel approach to bacterial neutralization.

A metallic foam is created when a mildly energetic composite includes a gasifying agent (GA). During a reaction the GA generates nucleation sites that promote the formation of bubbles. As the reaction wave passes, the gas pockets within the bubbles escape leaving a porous structure. In previous combustion synthesis studies, a GA may be added as a separate reactant usually in the form of a powder or granular material [11-13]. In this study, the metal oxide nanoparticles act as the GA in each mixture due to the low decomposition temperature associated with the nano-scale. Most previous work pertaining to the synthesis of porous materials using combustion synthesis was limited to micron-scale reactant particles. Tappan, et al. recently developed a new technique for the formation of a wide range of new nanoporous metals not currently accessible [14]. He demonstrated the ability to form foams of metals with differing chemistries and crystal structures including silver. The structural characteristics of the metal foams vary with composition and as a function of precursor chemistry and overpressure during combustion [14].

Self-propagating high-temperature synthesis (SHS) is used to create the metallic foams. The reactant particles are suspended in a solvent of hexanes and mixed using ultrasonic waves that break up macro-scale agglomerates. The final powder mixture is dried and cold-pressed in a uniaxial die to create cylindrical samples. The theoretical maximum density is calculated for each mixture as a weighted average of the pure solid densities of the constituent reactants (Al, Ag_2O, or TiO_2). Each sample contains 100 mg of reactant mixture and is cold pressed to a density of 70% of the theoretical value. The nanometer aluminum particles (nmAl) (NovaCentrix, Inc) with an average particle diameter of 50 nm are passivated with an average alumina shell 2 nm thick and used in the nano-scale samples. The 10 micrometer Al (micron Al) particles have an estimated 3 nm thick oxide shell and all metal oxide particles exhibit spherical

morphology and are used in the micron-scale samples. The Ag_2O is purchased from Sigma-Aldrich in two different sizes and has an average particle diameter of 30 microns and 100 nm. The TiO_2 is also purchased from Sigma-Aldrich and has an average particle diameter of 100 nm. Particle size, Al shell thickness and morphology information are provided by the suppliers. Each mixture is prepared for a stoichiometric equivalence ratio of 1.0.

For each sample set illustrated in Figs. 1 and 2, six samples are pressed and created through SHS before being exposed to bacteria. The samples are ignited using Nickel/Chromium wire that was fixed in spring tension along the sample's front face. The product microstructure is examined with a scanning electron microscope (SEM-Hitachi S-570) using a high-resolution stage at a voltage of 20 kV (Figure 1) and average porosity and pore size can be measured using mercury pycnometry with silwick as the wetting agent, which is a method analogous to hydrostatic weighing.

A 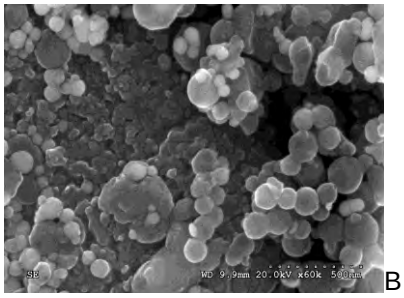 B 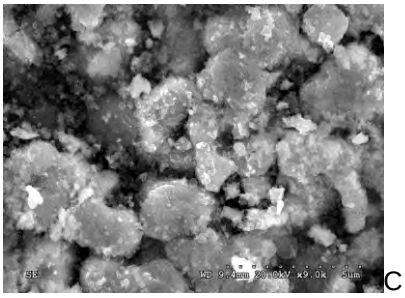 C 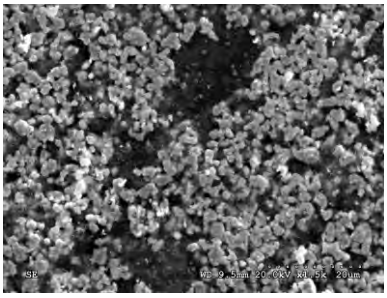

Figure 1: Scanning electron micrographs (SEMs) of Al-based metallic foams created through SHS A. nano Ag_2O, scale 500 nm, average pore size 100 nm ; B. nano TiO_2, scale 5 μm, average pore size 1 μm; C. micron Ag_2O, scale 20 μm, average pore size 5 μm

Experiments are performed to demonstrate the bacterial growth kinetics on synthesized foams. *Bacillus Subtilis* is a spore-forming bacterium like anthrax but benign [10] and used for this study. It was chosen because of its representative size and reactivity for several strains of dangerous bacteria [5]. The first experimental results are obtained for mixtures composed of Al/Ag_2O and Al/TiO_2. Experiments are also conducted on micron-scale Al/Ag_2O to examine the effect of the particle size on efficacy. The product foams are placed on an agar plate and 50 μL ($3.0x10^7$ CFU/ml at 0.1 ml) of *Bacillis subtilis* is collected with an Eppendorf research pipette and placed directly on and around the material while keeping the contact area consistent. The metallic foams are placed in an incubator for 24 hours at 37°C and then removed and checked for bacterial growth. The samples are then placed back into the incubator for another 24 hours and the results are shown in Figure 2. The bacterial growth is highlighted with a white circle. Figure 2C shows the control sample. Each sample is then swabbed and the bacteria remaining on the sample is re-incubated to determine bacteria kill.

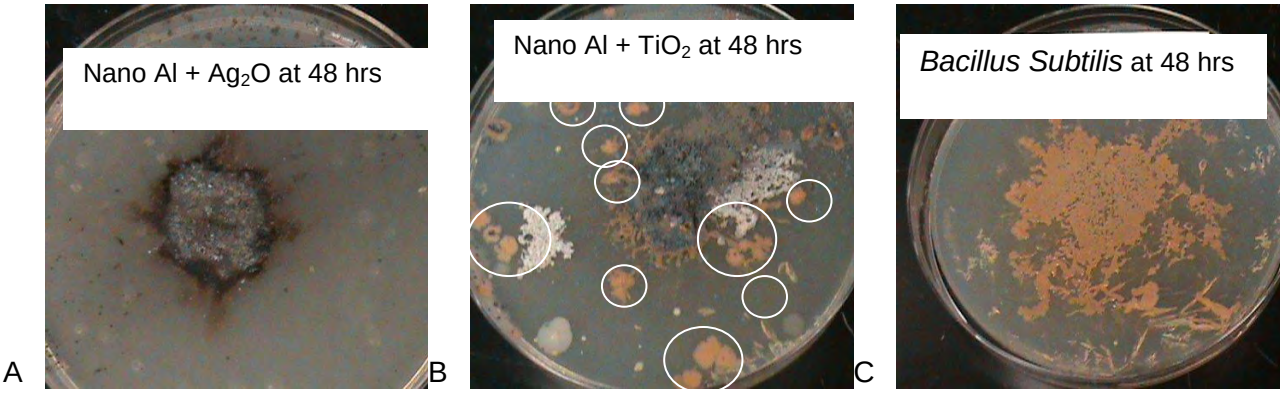

Figure 2: Al-based metallic foams after exposure A. nano Ag_2O; B. nano TiO_2; C. control

After 24 hours, there is no bacterial growth on the nano Ag_2O or nano TiO_2, but there is colony forming unit (CFU) growth areas on the micron Ag_2O nanofoam. Figure 2 is used to qualitatively

show that after 48 hours, there are significant CFUs on all of the foams, except for the nano $AlAg_2O$ which shows no sign of any bacteria. These results are consistent in all six samples. The micron samples do not delay or eliminate growth and thus are not shown here for comparison. Further experimentation shows that the bacteria are actually killed by the foam.

A Rigaku Ultima III X-ray diffractometer (40 kV, 44 mA, Cu Kα radiation) was employed for X-ray powder diffraction measurements (XRD) on the product materials for both particle sizes investigated.The specimens were scanned from 20.0 to 80.0 degrees in 0.15 second intervals at the resolution of 0.03 degrees and the results are shown in Figure 3.

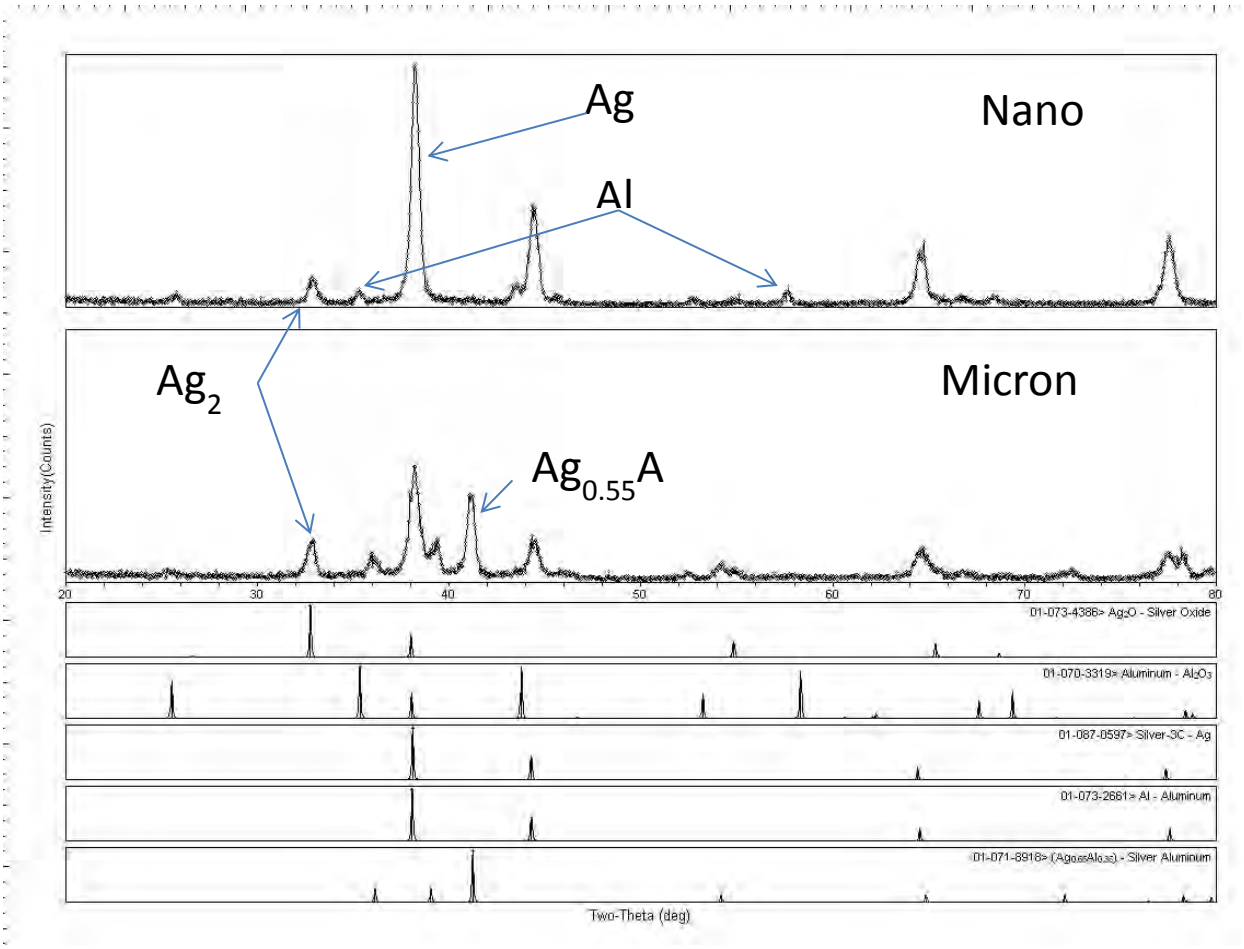

Figure 3: XRD of Nano and Micron Al+Ag_2O

These results give insight into the actual product composition of the metallic nanofoams. The nano Al+Ag_2O show significant percentages of Ag in the products while the micron Al+Ag_2O samples show high amounts of $Ag_{0.55}Al_{0.35}$. Of the metal ions, silver typically exhibits the highest toxicity for microorganisms and the least toxicity to animal cells depending on the system and cell lines. The antimicrobial spectrum of silver is extensive, including gram-negative aenterobacteria and gram-positive cocci [3]. When silver particles approach nano-scale dimensions they exhibit increased chemical activity due to their large surface to volume ratios and crystallographic surface structure [3-4]. The bactericidal properties of the nanoparticles are

size dependent, and initial studies on nanocrystalline silver confirm that their material structure is unique [2-8] leading to its effectiveness as an antifungal and antibacterial agent.

Five important conclusions can be drawn from these results. 1) Combustion synthesis can be used to create materials that have antibacterial properties. 2) Bacteria growth kinetics appear to be a function of reactant particle size. 3) Nanoscale reactants are more effective in neutralizing bacteria. 4) TiO_2 particles can delay, but not prevent bacterial growth, and; 5) metallic nanofoams composed of nano-scale Al and Ag_2O prevent growth of bacteria. These antibacterial metallic nanofoams can be easily created as a structural material or a metallic coating through combustion synthesis and have far-reaching applications in the food service and medical industry.

The authors would like to acknowledge support from DTRA *HDTRA1-10-1-0108* and program officer Dr. Suhithi Peiris and NSF *CBET-0914382* and program officer Dr. Phil Westmoreland.

REFERENCES

1. Vasilev K., Cook J., and Griesser H., "Antibacterial surfaces for biomedical devices," Expert Review of Medical Devices: 6, (5), 553-567; (2009).
2. Trapalis C., Kokkoris M., Perdikakis G., and Kordas, G., "Study of Antibacterial Composite Cu/SiO2 Thin Coatings," Journal of Sol-Gel Science and Technology," 26, 1213-1218, (2003).
3. Morones J.R., Elechiguerra J.L., Camacho A., Holt K., Kouri J.B., Ramirez J.T., Yacaman J., The bactericidal effect of silver nanoparticles, *Nanotechnology* 16: 2346-2353 (1998).

4. Zhao G., Stevens E., Multiple parameters for the comprehensive evaluation of the susceptibility of Escherichia coli to the silver ion, *Biometals* 11: 27-32 (1998).
5. Faille, C. et al. "Adhesion of Bacillus Spores and Escherichia coli Cells to Inert Surfaces: Role of Surface Hydrophobicity." *Canadian Journal of Microbiology* 48; 2002.
6. Kenar, L. et al. "Comparative Sporicidal Effects of Disinfectants after Release of a Biological Agent." *Military Science* 172(6) 2007.
7. Whitney, E. et al. "Inactivation of Bacillus anthracis Spores." *Emerging Infectious Diseases* 9(6); 2003.
8. Taylor P.L., Ussher A.L., Burrell R.E., Impact of heat on nanocrystalline silver dressings Part I: chemical and biological properties, *Biomaterials* 26: 7221-7229 (2005).
9. Fujishima A., OhkoY., Saitoh S., Tatsuma T., Niwa C., and Kubota Y., "Antibacterial and Anticorrosion Effects of Titanium Dioxide Photoactive Coatings," http://www.electrochem.org/dl/ma/201/pdfs/0053.pdf.
10. Whitney, E. et al. "Inactivation of Bacillus anthracis Spores." *Emerging Infectious Diseases* 9(6); 2003.
11. Hunt EM, Pantoya ML and R J Jouet "Combustion Synthesis of Metallic Foams from Nanocomposite Reactants," *Intermetallics* vol. 14 (6), pp. 620-629 (2006).
12. Kistler S.S., Coherent expanded aerogels in jellies, *Nature* 127: 741 (1931).
13. Walsh D., Arcelli L., Toshiyuki I., Tanaka J., Mann S., Dextran templating for the synthesis of metallic and metal oxide sponges, *Nature Mater.* 2: 386-390 (2003).
14. B. C. Tappan,* M. H. Huynh, M. A. Hiskey, D. E. Chavez, E. P. Luther, J. T. Mang, and S. F. Son, "Ultralow-Density Nanostructured Metal Foams: Combustion Synthesis,

Morphology, and Composition," Contribution from the Los Alamos National Laboratory, Los Alamos, New Mexico 87545 *J. Am. Chem. Soc.*, 2006, 128 (20), pp 6589–6594.

Spore Deactivation Conditions Necessary for Millisecond Dwell Times

Oliver Mulamba[1], Emily M. Hunt[2] and Michelle L. Pantoya[1*]

[1]*Mechanical Engineering Department, Texas Tech University, Lubbock, TX 79409*

[2]*Mechanical Engineering Department, West Texas A&M University, Canyon, TX 79016*

*Corresponding author. Mailing address: Corner of 7th and Boston Ave, Mechanical Engineering Department, Texas Tech University, Lubbock, TX 79409-1021, Phone: 806-742-3563, Electronic mail: michelle.pantoya@ttu.edu

Abstract

Composite energetic materials that include biocidal agents have recently spurred interest for their potential to deactivate spore forming bacteria. We have examined the feasibility of this approach using bacterial spores that include bacillus thuringiensis and bacillus anthracis exposed to energetic formulations that include iodine, such as aluminum and iodine pentoxide (Al-I_2O_5). These fundamental studies resulted in an understanding that a balance of two primary reaction parameters needs to be coupled in order to reduce dwell times: temperature and the production of iodine gas. However, those studies examined spore neutralization on the order of minutes while the current impetus is to deactivate spore forming bacteria within milliseconds. Towards this end, the results from previous studies have been extrapolated to the millisecond time regime in an effort to identify the potential reaction conditions that will ensure deactivation. The Pearson product-moment correlation confirmed linear dependence of the data prior to the extrapolation and results show that the coupled thermal-biocidal gas mechanism will require elevated temperatures of 360^{o}C and allow for 80% deactivation in tens of milliseconds while thermal conditions alone would require nearly 1000^{o}C for the same deactivation.

Key Words: *biological warfare, energetic materials, bacillus thuringiensis, iodine, combustion*

Methods

Iodine gas alone was shown to have no effect on deactivating BT spores, but a combination of elevated temperatures in the range of 110 and 120^{o}C coupled with iodine gas were successful at deactivating BT over a period of 15 minutes [1]. While this study aids in understanding the fundamental parameters influencing spore deactivation, accelerating deactivation to the millisecond time regime will require manipulation of these parameters. The reader is referred to [1] for details of that experiment. The data for the coupled and uncoupled 110 and 120^{o}C cases are presented in Fig. 1. A fifth-order polynomial fit was applied to each set of data to produce individual trend-line equations.

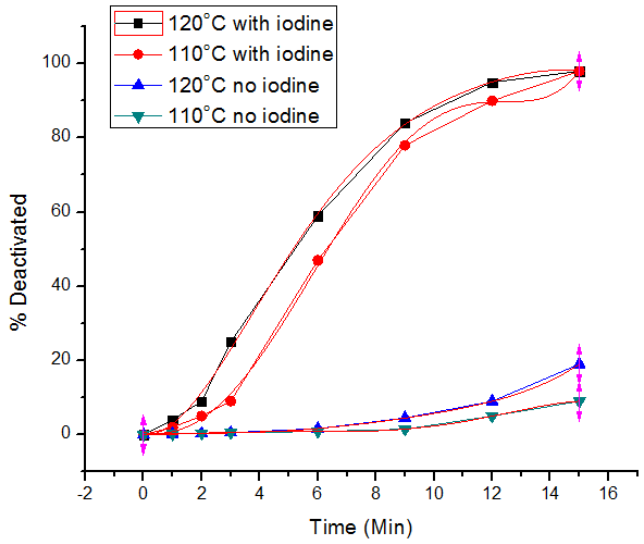

Figure 1. Polynomial plots of the deactivation data with and without iodine

The Pearson product-moment correlation coefficient (PPMCC) is a statistical method that provides a measure of linear dependence or correlation between two varying sets of data [2, 3]. The correlation measure is assigned as a value between +1 and -1; +1 implying that a linear equation perfectly describes the relationship between the two data sets while -1 implies otherwise. The PPMCC was calculated for the two data sets containing iodine and the two without iodine. The data set with iodine had a PPMCC value of 0.9914 and the data with no iodine showed a higher linear value of 0.9945. Given that both values are relatively close to 1, assumption of a linear relationship between the two data sets is reasonable for both conditions with and without iodine.

With the PPMCC allowing a linearity assumption, this analysis is then focused on the ms time regime. The data in this range is interpolated to include 100 points, aiding to increase the accuracy of following calculations. These data points are then fitted with the fifth-order polynomial. The coefficients of the acquired trend-lines are used to extract linear correlation constants for the data sets with no iodine as well as the iodine containing set. For example, if Eqs. (1) and (2) represent two fifth-order curve fits, based on assumed linearity, a linear correlation constant P_i could be determined from Eq. (3). For Eqs. (1) and (2), a_i and b_i are constants of the indexed (i) order.

$$Y_1 = a_1t + a_2t^2 + a_3t^3 + a_4t^4 + a_5t^5 + a_6 \quad (1)$$

$$Y_2 = b_1t + b_2t^2 + b_3t^3 + b_4t^4 + b_5t^5 + b_6 \quad (2)$$

$$Y_2 \cong P_iY_1 \quad (3)$$

The two temperatures analyzed (i.e., see Fig. 1: 110 and 120^{o}C) have a 10 degree difference, the correlation constant P_i is therefore a function of 10^{o}C for the non- iodine data set

as well as the included iodine data set. Therefore, this leads to a base equation for both the 110°C no iodine and iodine data sets shown in Eq. (4)

$$Y = P_f(a_1t + a_2t^2 + a_3t^3 + a_4t^4 + a_5t^5 + a_6) \quad (4)$$

where Y is the percent deactivation (y-axis in Fig. 1), P_f is the linear correlation constant, a_i are known coefficients from the polynomial fit and t represents the time in seconds. It is noted that P_f is an unknown in Eq. (4). Values for P_f can be calculated for a specified amount of Y deactivation at time t and using Eq. (5) the temperature change related to the P_f constant can be determined.

$$\frac{P_f}{P_i} = \frac{\Delta T_f}{\Delta T_i} \quad (5)$$

In Eq. (5), ΔT_i is the 10°C associated with P_i. Once ΔT_f is determined it is added to the base temperature $T_i = 110^oC$ to provide the final temperature.

Results

Figure 2 shows results from calculations that estimate temperatures required to perform at least 80% deactivations.

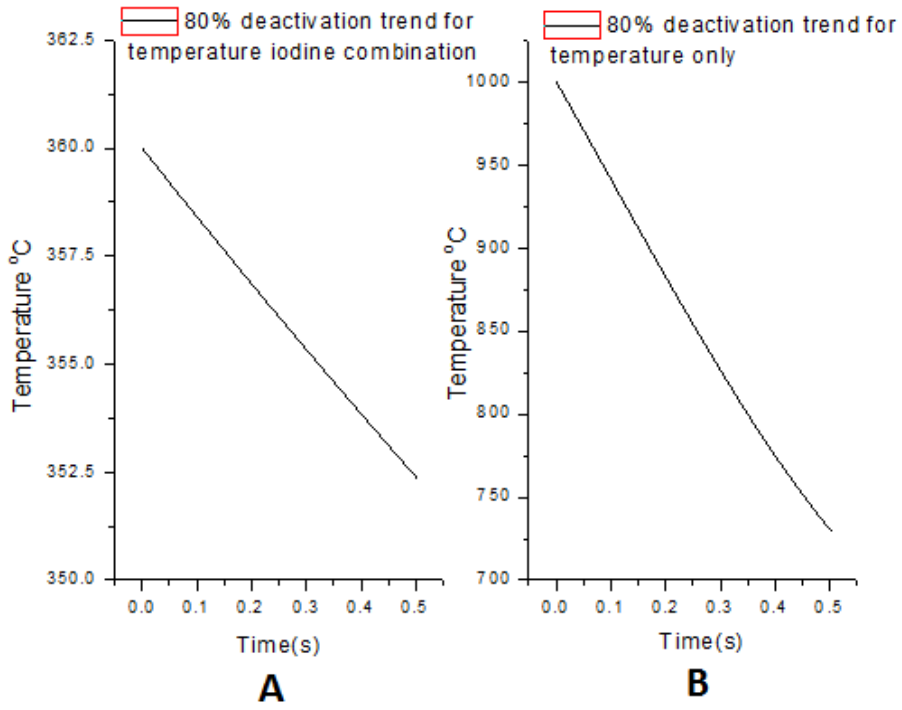

Figure 2. Plots of estimated millisecond range deactivation behavior A. with iodine and temperature coupled mechanism and B. with elevated temperature only.

Discussion

The extrapolation analysis reveals that a temperature of around 360 ^{o}C would be required for 80% deactivation in the initial millisecond range. This is significantly lower than the calculated values for isolated temperature of 1000°C, which in fact correlate with heat data in literature [4].

It should be noted that the energetic formulations such as Al-I2O5 [5, 6], AlI_x [7, 8], and Al-AgIO [9] all produce locally isolated elevated temperatures, localized near the source. The spatial distribution of temperature from any of these composite energetic materials has been documented to exponentially decrease with distance from the reaction [10]. Using these formulations for these biocidal applications would require additives to the formulation that would increase the spatial distribution of temperature or perhaps influence the permeability of the spore such that biocidal gas transport can be accelerated. Other contributing factors not examined here include pressure waves from detonating mixtures. In unconfined settings, these candidate formulations deflagrate such that pressure influences are negligible. However, confining these mixtures or adding explosives may facilitate compression waves that may also contribute to deactivation.

Conclusions

In the pursuit of millisecond dwell times with minimal energy requirements, it is estimated that using a combination of elevated temperature and iodine gas would be an effective approach requiring a minimum temperature of 360^{o}C that would allow for 80% BT spore deactivation. In contrast, elevated temperatures alone would require 1000°C to accomplish the same deactivation.

Acknowledgements

The authors are grateful for the financial support received from the Defense Threat Reduction Agency (DTRA) on this project and the encouragement and support of our program manager, Dr. Suhithi Peiris.

References

[1] Mulamba, O., Pantoya, M.L., Hunt, E.M., Permeability acclimatization responsible for dwell time reductions in spore deactivation, Submitted to the *Journal of Applied Molecular Biology*, May 2012.

[2] Rodgers, J. L., Nicewander, W. A., Thirteen ways to look at the correlation coefficient, *The American Statistician*, 42(1):59–66, 1988.

[3] Stigler, S. M., Francis Galton's Account of the Invention of Correlation. *Statistical Science* **4** (2): 73–79, 1989.

[4] C. A. Alexander, J. S. Ogden, M. A. LeVere, C. F. Dye, and D. F. Kohler, "Thermal Deactivation of Aerosolized Bacteria," Defense Threat Reduction Agency, Technical Report 1998.

[5] Clark, B. R. and Pantoya, M. L., the aluminum and iodine pentoxide reaction for the destruction of spore forming bacteria, *Physical Chemistry Chemical Physics* 12(39); 12653-12657, 2010.

[6] Farley, C., Pantoya, M.L., Reaction Kinetics of Nanometric Aluminum and Iodine Pentoxide, *Journal of Thermal Analysis and Calorimetry* 102(2), 609-613, 2010.

[7] Zhang, S., Schoenitz, M., Dreizin, E. L., Iodine release, oxidation, and ignition of mechanically alloyed Al-I composites, *Journal of Physical Chemistry C* 114(46), 19653-19659, 2010.

[8] Zhang, S., Badiola, C., Schoenitz, M., Dreizin, E. L., Oxidation, ignition, and combustion of AlI2 composite powders, *Combustion and Flame* 159(5), 1980-1986, 2012.

[9] Sullivan, K.T., Piekiel, N.W., Chowdhury, S., Wu, C., Zachariah, M.R., Johnson, C.E., Ignition and combustion characteristics of nanoscale Al/AgIO3: A potential energetic biocidal system, *Combustion Science and Technology* 183(3), 285-302, 2011.

[10] Glumac, N., Krier, H., Bazyn, T., Ever, R.,Temperature measurements of aluminum particles burning in carbon dioxide, *Combustion Science and Technology* 177(3), 485-511, 2005.

Permeability acclimatization responsible for dwell time reductions in spore deactivation

Oliver Mulamba[1*], Michelle L. Pantoya[1] and Emily M. Hunt[2]

[1]*Mechanical Engineering Department, Texas Tech University, Lubbock, TX 79409*

[2]*Mechanical Engineering Department, West Texas A&M University, Canyon, TX 79016*

*Corresponding author. Mailing address: Corner of 7th and Boston Ave, Mechanical Engineering Department, Texas Tech University, Lubbock, TX 79409-1021, Phone: 806-742-3563, Electronic mail: okmulamba@yahoo.com

Abstract

The increase in the threat of biological warfare has led to an increase in research directed toward methods of neutralizing spore forming bacteria. One approach takes advantage of the chemistry and exothermic energy from a thermite reaction as a means for the deactivation of bacterial spores. The spore's neutralization upon exposure to a thermite reaction may be explained by increased permeability within the spore structure due heat transfer and biocidal chemistry resulting from the reaction temperature and generated gas.

The objective of this work is to fundamentally examine the components enabling deactivation of *Bacillus thuringiensis*. The deactivation is attributed to the thermal effect of the heat on the spore and the associated chemical effect of halogen gas (i.e., produced from thermite combustion). Results show heat transfer in the spore enhances the effectiveness of the halogen gasses in the deactivation process and that elevated temperatures increase spore permeability, facilitating gas penetration and accelerating spore deactivation. These results provide molecular-level insights into the components underpinning biological processes leading to spore neutralization.

The results of this study lay the foundation upon which the efficiency of thermite bacterial deactivation may be improved. Analyses of dwell times reveal parameters directly affecting bacterial deactivation when utilizing both heat and biocidal iodine gas. This knowledge being previously related to biocidal solutions only and not gasses. Yet, gas generation and dispersion may be an important method for improving spatial neutralization of biocidal agents, especially those related to mass bacterial spore destruction.

Introduction

The destructive possibilities of anthrax as a biological weapon have been observed in a number of different situations, from the 1979 Moscow incident to the Tokyo attacks in 1993 (Inglesby et al., 1999). The threat of biological warfare is a very real possibility with several countries now undertaking research to improve and strengthen their attack and defense strategies (Inglesby et al., 1999). One event that directly affected the United States of America was observed in the 2001 "letter attacks". That event claimed the life of 5 individuals and contaminated 22 others (Kournikakis et al., 2011). Recently various methods have been studied for the sole purpose of neutralizing this threat via biocidal solutions, pressure and temperature (Kida et al., 2004, Clery-Barraud et al., 2004).

A contrasting path made use of thermite combustion as an effective neutralization tool. The most effective reaction is composed of aluminum (Al) fuel and iodine pentoxide (I_2O_5) oxidizer (Clark and Pantoya, 2010). This reaction generates iodine gas, which is a different phase to the effective biocidal iodine solutions that have been thoroughly observed (Pennell et al., 2008, Lee et al., 2008, Kida et al., 2004). Initial studies showed that Al-I_2O_5 was effective in deactivating *Bacillus* spores, with dwell times in the 45 min-1 hr range (Clark and Pantoya, 2010). Deactivation (or neutralization) as defined here is destroying the ability of a spore to grow and form colonies. *Bacillus thuringiensis* is used as the testing medium in this work. Rice et al.(2005) found that *Bacillus thuringiensis'* behavior and reaction to chemical and thermal attacks closely resembled *Bacillus anthracis* behavior, therefore *Bacillus thuringiensis* was used in this work as an appropriate surrogate in place *Bacillus anthracis*.

The deactivation effectiveness of Al-I_2O_5 is theorized to be primarily based on a combination of two parameters: iodine gas generation and thermal energy generation. High temperatures have been observed to effectively deactivate spores (Mullican et al., 1971, Alexander et al., 1998). However, high temperatures generated by a thermite reaction are typically highly localized to the reaction site and do not propagate significantly high temperatures beyond the reactants. Thermal wave propagation of a thermite reaction show exponential temperature decreases in temperature with distance from the reaction (Bazyn et al., 2007). These observations imply that to achieve effective observations with the use of thermites, iodine gas generation would need to participate sizably in the deactivation process.

The objective of this study is to understand the components preceeding and enabling the deactivation of *Bacillus thuringiensis* spores, with variable temperature and iodine gas treatements. This is accomplished by experiments that isolate and focus on the effects of temperature, iodine gas and the combination of the two parameters, allowing for quantifiable comparisons between treatments and analysis of the efficacy of deactivation.

MATERIALS AND METHODS

Previous thermal related studies involving bacterial spores show that for quantitatively significant results, the setup should have the spores surrounded by heat, in a medium allowing for fast heat transfer (Clery-Barraud et al., 2004, David and Merson, 1990, Mullican et al., 1971). Based on this understanding a biocidal exposure chamber (BEC) was designed, as shown in Fig.1. The BEC is composed of 2 vials made of thin glass, allowing for rapid and even distribution of temperature. The BEC allows for direct interaction of the biocidal gas with the *Bacillus* spores, which are dried onto the bottom of the top vial as illustrated in Fig. 1. The vials were purchased from Wheaton and the iodine crystals were purchased from Sigma Aldrich. Iodine crystals were used to supply the iodine gas for the deactivation tests. In order to produce equal concentrations of iodine gas in each test, 25mg of iodine crystals were used in each container. Tests indicated that 25 mg of crystal would fully sublimate in the allotted time of testing, therefore allowing for equality in gas concentrations for each controlled volume test. This study first isolates the effects of temperature, then iodine gas and then examines the combined effect of temperature and iodine gas on the spores.

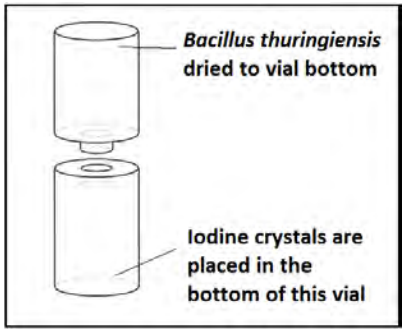

Fig. 2 Biocidal exposure chamber (BEC) consisting of two attached vials

Bacteria Preparation

Bacillus thuringiensis was purchased from Raven Labs with a concentration of $3.0x10^7$ CFU/ml. A 0.1ml sample is collected with an Eppendorf research pipette and placed in the top portion of the BEC. The solution in the vial is left to evaporate at 37^oC for 12h inside a Quincy Labs incubator. This process leaves the surface of the vial covered with the dried spores which are then ready for further experimentation.

Experimental procedures

Temperature based tests:

Post bacteria preparation, the vial is connected to the secondary part of the BEC, containing the iodine crystals. These BECs are placed within an Imperial V Laboratory oven at different temperatures for varying times, as shown in Table 1. The iodine gas is produced from the sublimation of the iodine crystals. The BECs vary, a portion of them contain iodine crystals while the others do not. This enables isolation of temperature effects as compared to the combined effects of the iodine gas and temperature.

Table 1 Matrix of experimental conditions for iodine and non-iodine containing BECs

Exposure time (min)	Temperature (^oC)
15:30:45	70
15:30:45	80
15:30:45	90
15:30:45	100
15:30:45	110
15:30:45	120
15:30:45	130

Iodine based tests:

When performing the iodine only tests, a hotplate was used instead of the oven. The hotplate was set to the same temperatures as the temperature based tests, as shown in Table 1, to keep the iodine gas production constant for all tests. Since the basis of the iodine tests is to focus solely on the effects of iodine, it was necessary to limit heat transfer to the vial containing the dried spores. An Acrylonitrile butadiene styrene (ABS) divider was placed between the vials as shown in Fig. 2, allowing for limited heat transfer to the top vial.

Fig. 3 BEC with ABS divider

Analysis

Post exposure to the deactivation agents, the BECs containing the *Bacillus* spores were rehydrated by adding 0.1ml of distilled water followed by 5min shaking on a Vortex Genie-2 mix, to assist in the recovery of all dried spores. Once the spores are re-suspended in the distilled water, they are drawn out and deposited onto Lysogeny Broth (LB) agar plates purchased from Sigma Aldrich. These plates are then placed into an incubator at 37^{o}C for 24hr, removed to be photographed and then replaced for a further 24hrs after which the agar plates are again photographed. Colony growth is not expected to continue past 48hrs and that is the reason for the allotted incubation time. The basis of a quantifiable measure of deactivation lies in comparing the exposed sample to a control sample. This is performed using colony counts and covered surface area measurements, allowing for increased accuracy. The deactivation ratio (*DR*) is computed using Eq. (1)

$$DR = \frac{Test\ \#}{Control\ \#} \quad (1)$$

where *Test#* and *Control#* are the colony counts and surface areas retrieved from the tested sample and control sample. The deactivation percentage (*DP*) is calculated using Eq. (2).

$$DP = (1 - DR) * 100\% \quad (2)$$

This approach is similar to the viability loss method used by other investigators (Jung et al., 2009, Lee and Lee, 2006). Microbial deactivation in microbiology studies use log reduction for quantifying purposes. In relation to our more engineering perspective, if $1/DR = 100$, this would be referred to as a 2 log reduction using the log reduction method.

Spore structure

Dormant *Bacillus* spores are more resistant to strenuous treatments than their biologically active counterparts (Bloomfield and Arthur, 1994, McDonnell and Russell, 1999). The resistance of a spore to strenuous treatment and other types of attacks is dependent on a variety of factors, including spore structure and chemical composition(Setlow, 1995). Understanding the makeup of the spore will aid in better comprehending the response to strenuous situations. Fig. 3 shows a simplified 3-dimensional image of a spore illustrating the different layers making up the spore.

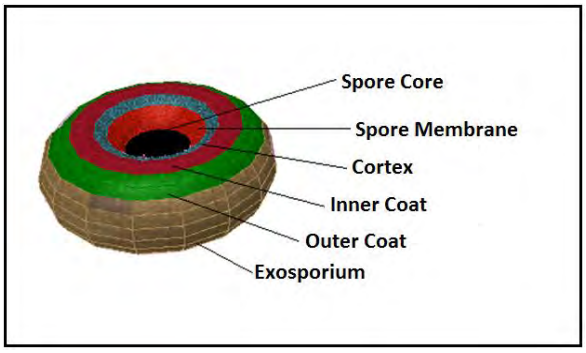

Fig. 4 Simplified 3D depiction of spore layers

The *Bacillus thuringiensis* spore has as its outer most layer, the exosporium (Gerhardt et al., 1976). This is not standard for all spores as some (e.g., *Bacillus subtilis*) do not have an exosporium or they are very small in size. The exosporium may be viewed as an extension from the coat layer beneath it. This is based on work that found that this layer contains proteins

specific to the coat beneath it (Todd et al., 2003, Lai et al., 2003). The makeup of the exosporium includes proteins and glycoproteins specific to exosporiums, and even though function of this layer and associated proteins are not yet known, they are believed to be important in interactions with other organisms(Redmond et al., 2004, Todd et al., 2003).

The layer internal to the exosporium is the spore coat, which is separated to an inner and outer coat. It is made of several structurally complex layers, with a loose fitting, granular outer spore coat and a laminated inner spore coat(Gerhardt et al., 1976). The spore coat is believe to be composed of at least 70 proteins (McKenney and Eichenberger, 2012). The functions of the proteins are mostly unknown, but some are known to be morphogenic and dealing with the assembly of the spore (McKenney and Eichenberger, 2012, Lai et al., 2003, Bailey-Smith et al., 2005).

The spore coat is believed to play a vital role in spore resistance to certain chemical attacks. This is vital in protecting the cortex from interactions with chemicals that can cause cortex degradation, and possibly prove lethal to the spore (Tennen et al., 2000, Driks, 1999). This layer apparently shows no resistance to radiation and heat and even though it is known to be resistant to some chemicals, there are chemicals to which it has no resistance(Driks, 1999). Internal to the spore coat is the cortex and this layer is composed of peptidoglycan (PG)(Zhang et al., 2012). Dormant spore formation requires reduction in the water content of the spore core, and this vital role is performed by the cortex. During germination the spore core expands and to allow for this germination process the cortex is degraded(Setlow, 2003). The spore membrane lies internal to the cortex and is a main defensive layer, protecting the spore DNA from damage (Tennen et al., 2000). It is a high permeability layer that acts as a barrier attempting to keep out chemicals and other potential dangers from getting to the spore core (Nicholson et al., 2000, Tennen et al., 2000).

At the center of the spore lays the spore core containing the DNA, tRNAs, most enzymes and ribosomes (Gerhardt et al., 1976, McKenney and Eichenberger, 2012). Three molecules exist within the spore cores that are believed to play a role in its defensive attributes (Fernandez et al., 1994, Griffith et al., 1994, Paidhungat et al., 2000). These are:

1. Small Acid-soluble Spore Proteins (SASP) of the α/β-type
2. Water
3. Dipicolinic Acid (DPA).

The α/β-type SASP exist solely in the spore core where they saturate the DNA and factor significantly in its resistance to chemicals and heat (Genest et al., 2002, Tennen et al., 2000). Macromolecular movement is restricted in the core due to low amounts of free water. Around 30-50% wet weight of the core is made up of water and this low water content is believed to play an important role in regard to resistance against wet heat (Gerhardt and Marquis, 1989). DPA is located in the spore and comprises 5-15% of the spore's dry weight. The low water content in the core is in part attributed to the large presence of DPA(Gerhardt and Marquis, 1989).

RESULTS

Temperature

Tests were conducted to locate the range of temperatures at which deactivation would occur for the setup used. These were conducted in two ways: observing response based on just temperature and observing response based on combined effects of iodine gas and thermal exposure. Figure 4 presents a superimposition of the two output graphs. The temperature graph shows no significant deactivation in the range from 60-110 °C, yet past 115 °C increases were observed. Beyond 120 °C sizeable deactivation is observed. These results were based on dwell times of 15minutes and were repeated 3 times for repeatability and accuracy. Comparing the two graphs, there is a disparity observed in regard to the temperatures at which deactivation begins. It appears that the addition of iodine gas results in a sizeable reduction in the deactivation temperature.

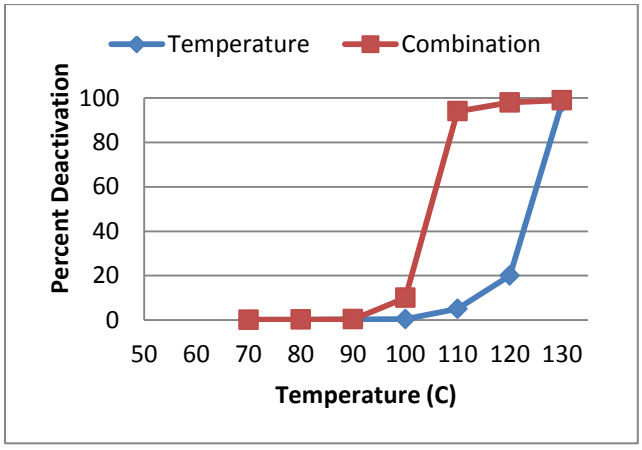

Fig. 5 Superimpositions of deactivation trends

Exposure time

Further tests were performed in order to assess the influence of dwell time, defined here as the exposure time of the spore to the environment (i.e., thermal and/or chemical). Exposure times were varied up to 15 minutes and results are shown in Fig. 5. Included in these results is exposure of the spores to just the iodine gas with no thermal aspect present (see Fig. 5a). It is interesting to notice that in Fig. 5b, there appears a lag time associated with the onset of deactivation. Another observation is that a slight increase in temperature shortens this lag time thereby accelerating the onset of spore deactivation.

a.

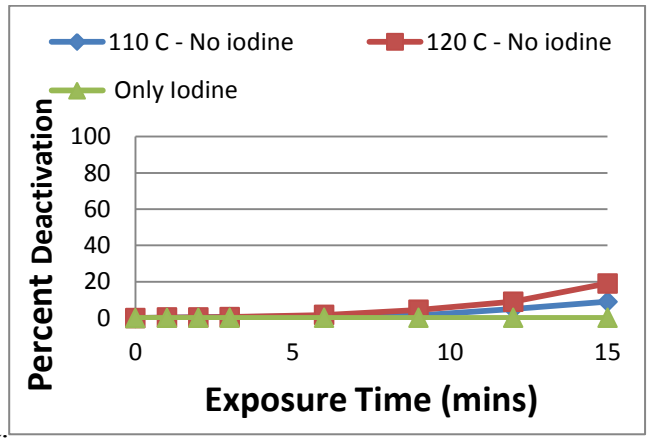

b.

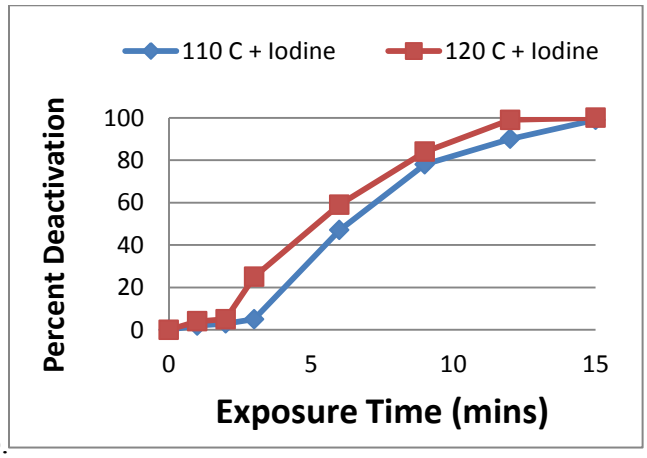

Fig. 6 Percent *Bacillus thuringiensis* deactivation as a function of exposure time. a. Samples exposed to individual thermal and chemical environments and b. Samples exposed to a thermal/chemical combined environment

Discussion

Mechanisms of deactivation

Prior to discussing the results it is important to understand the means by which the deactivating agents achieve their purpose. Even though the specific nature of damage remains unknown, dry heat related deactivations have been found to be responsible for DNA damage(Setlow, 2005). Deactivation due to iodine in solution has been characterized as one of the following intertwined observations. The iodine in solution is believed to either inactivate the corticolytic enzymes responsible for cortex degradation during germination, or alter the cortex structure such that it does not degrade during germination (Miyata et al., 1997, Tennen et al., 2000).

Observations

Existing theories applied to studies involving iodine in solution can be considered here to explain the behaviors observed in Figs. 4 and 5. For example, research has shown that *Bacillus thuringiensis* has an inherent thermal defense mechanism embedded into its structure in order to thermo-regulate itself and protect its vital proteins which lie in its protoplast (see Fig. 3) (Alexander et al., 1998). Thermal regulation within the spore is achieved by retaining liquid (i.e., water) in the outer layers of its core (Hoffman et al., 1968, Drummond and Pflug, 1970, Alexander et al., 1998). Indeed it is literary fact that spores have water content; yet this theory may not apply here because our study employs dried spores whereas [10, 36-37] studied wet spores. With dry spores, the intrinsic water content is minimal, and the balance of the amount of water versus the amount of heat would not produce the same observed effects.

A second useful theory is based on the observed lag times. Similar lag times associated with deactivation have been observed for tests using biocidal solutions (Russell, 1996, Larson and Marinas, 2003, Corona-Vasquez et al., 2002). The reasons for this lag were initially not known but the results showed the lag time shortened with increase in temperature (Corona-Vasquez et al., 2002, Larson and Marinas, 2003). A mathematical model was developed by Fernando et al. (Fernando and Othman, 2006) based on solute concentration as the factor controlling lag time. A critical iodine in solution concentration was determined before deactivation can begin, therefore explaining the lag. Their analyses [41] was based on similar concentration related observations (Watson, 1908). An equation was developed based on this

model which held relatively true for biocide solutions and their effects on bacteria (Fernando and Othman, 2006). The initial hypothesis may be to assume the same model could be applied to biocidal gas, and not just biocidal solutions. However, this theory does not hold for biocides in the gaseous phase according to Fig. 5a. We see that even when using the same concentrations of iodine, when there is no temperature involved, no deactivation effects are observed as compared to the combination results. Therefore the concentration of iodine gas alone does not influence deactivation and some other explanation is needed to for the lag time in these gaseous studies.

We propose a third theory. The essence of the spore is multiple layers of proteins lying on top of one another. The spore is known to be a porous medium (Russell, 1998, Gerhardt et al., 1976, Setlow, 2005). We suggest viewing the pores within the spore as a network of conduits as modeled by Dullien (1979, 181-190) and shown in Fig. 6a (Kaviany, 1995).

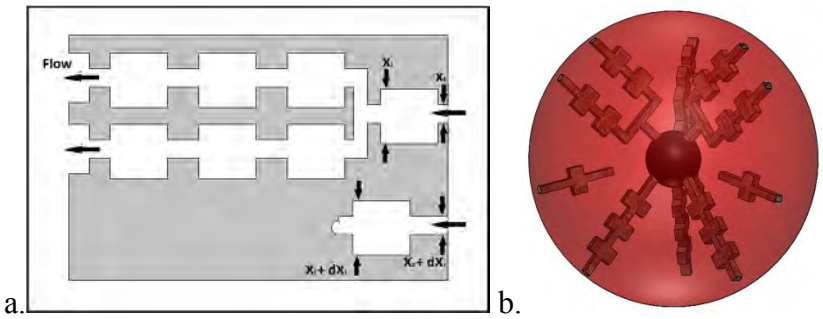

a. b.

Fig. 7 Networks of conduit a. 2-D, b. 3-D

Fig. 6b shows a simplified version of what this may look like in a 3 dimensional visual, with the spore core as the center sphere. This would present a fair representation based on the fact that the spore, like the Dullien model, has variant pore-size distributions. Literature shows that temperature increase causes structural changes in proteins (Tommasi et al., 2009, Heremans and Smeller, 1998, Tilton et al., 1992). These volume affecting changes have been attributed to an increase in the porosity of the proteins (Tilton et al., 1992, Tommasi et al., 2009). The Dullien model offers an equation to calculate the permeability of a three dimensional network using: the Darcy law, the Hagen-Poiseuille equation and the cumulative pressure drop [44] as in Eq. (3).

$$K = \frac{\epsilon}{96}\sum_i \frac{S_i(\sum_j {}^{V_{ij}}/_{d_j^2})^2}{\sum_j V_{ij}(\sum_j {}^{V_{ij}}/_{d_j^6})} \quad (3)$$

In Eq. (3), i = 1,2,3 represents the three orthogonal coordinate axes and j = 1,2,…,N is the index for the capillary segment j; S_i represents the pore volume of the medium represented by the component network i; $V_{ij} = (\pi/4)d_j^2 l_{ij}$, where d_j is the diameter of the segment j; and l_{ij} = capillary segment length j in the i direction (Kaviany, 1995). We want to draw attention to ϵ which is representative of porosity. What is deduced from this is that an increase in the porosity of this system results in an increase in the permeability. Literature shows that for proteins, an increase in temperature causes an increase in porosity and relating this to the Dullien model equation, Eq. (3) , the porosity increase relates to an increase in permeability(Tilton et al., 1992, Tommasi et al., 2009).

Our hypothesis therefore is that in relation to the deactivation of *Bacillus thuringiensis* using gaseous iodine and temperature, improved deactivation rates are based on an increase in spore permeability which allows the iodine particle to reach its point of destruction faster (i.e., cortex), and this is simultaneously supported by the temperature's deactivation effects on the core. Not only is the permeability increased but the temperature change will increase the kinetic energy of the biocidal gas. This is based on the average molecular kinetic energy which can be described in Eq. (4).

$$\frac{mV^2}{2} = \frac{3}{2}kT \quad (4)$$

In Eq. (3), m is mass, V is velocity, k is the Boltzmann constant and T is temperature (Serway and Jewett, 2004). This increase in gas temperature will increase the velocity and mass transfer rate of gas into the spore. This lines up accurately with the observed results and provides an understanding of the manner of deactivation using iodine gas and temperature as opposed to iodine solutions.

Conclusion

The results suggest a synergistic behavior between the iodine gas and temperature in the deactivation of *Bacillus thuringiensis*. Due to the modes of deactivation this synergistic behavior

may be beneficial in the reduction of dwell times. In regard to thermite reactions and their thermal propagation gradient, this knowledge would prove useful in potentially improving deactivation efficiency. The results suggest a thermite reaction with increased spatial temperature distribution and slow burning characteristics could potentially show sizable improvements as a spore neutralization medium.

Acknowledgements

The authors are grateful for the financial support received from the Defense Threat Reduction Agency (DTRA) on this project and the encouragement and support of our program manager, Dr. Suhithi Peiris.

References

ALEXANDER, C. A., OGDEN, J. S., LEVERE, M. A., DYE, C. F. & KOHLER, D. F. 1998. Thermal Deactivation of Aerosolized Bacteria. Defense Threat Reduction Agency.

BAILEY-SMITH, K., TODD, S. J., SOUTHWORTH, T. W., PROCTOR, J. & MOIR, A. 2005. The ExsA protein of *Bacillus cereus* is required for assembly of coat and exosporium onto the spore surface. *Journal of Bacteriology,* 187**,** 3800-3806.

BAZYN, T., GLUMAC, N., KRIER, H., WARD, T. S., SCHOENITZ, M. & DREIZIN, E. L. 2007. Reflected shock ignition and combustion of aluminum and nanocomposite thermite powders. *Combustion Science and Technology,* 179**,** 457-476.

BLOOMFIELD, S. F. & ARTHUR, M. 1994. Mechanisms of Inactivation and Resistance of Spores to Chemical Biocides. *Journal of Applied Bacteriology,* 76**,** S91-S104.

CLARK, B. R. & PANTOYA, M. L. 2010. The aluminium and iodine pentoxide reaction for the destruction of spore forming bacteria. *Phys Chem Chem Phys,* 12**,** 12653-7.

CLERY-BARRAUD, C., GAUBERT, A., MASSON, P. & VIDAL, D. 2004. Combined effects of high hydrostatic pressure and temperature for inactivation of *Bacillus anthracis* spores. *Appl Environ Microbiol,* 70**,** 635-7.

CORONA-VASQUEZ, B., SAMUELSON, A., RENNECKER, J. L. & MARINAS, B. J. 2002. Inactivation of *Cryptosporidium parvum oocysts* with ozone and free chlorine. *Water Res,* 36**,** 4053-63.

DAVID, J. R. D. & MERSON, R. L. 1990. Kinetic-Parameters for Inactivation of *Bacillus-Stearothermophilus* at High-Temperatures. *Journal of Food Science,* 55**,** 488-&.

DRIKS, A. 1999. *Bacillus subtilis* spore coat. *Microbiology and Molecular Biology Reviews,* 63**,** 1-+.

DRUMMOND, D. W. & PFLUG, I. J. 1970. Dry-heat destruction of *Bacillus subtilis* spores on surfaces: effect of humidity in an open system. *Appl Microbiol,* 20**,** 805-9.

FERNANDEZ, P. S., OCIO, M. J. & MARTINEZ, A. 1994. Relation between Thermal-Resistance and Dpa Content in Variants of the Same Strains of Bacillus-Stearothermophilus Spores. *Letters in Applied Microbiology,* 19**,** 118-120.

FERNANDO, W. J. & OTHMAN, R. 2006. Relevance of diffusion through bacterial spore coats/membranes and the associated concentration boundary layers in the initial lag phase of inactivation: a case study for Bacillus subtilis with ozone and monochloramine. *Math Biosci,* 199**,** 175-87.

GENEST, P. C., SETLOW, B., MELLY, E. & SETLOW, P. 2002. Killing of spores of *Bacillus subtilis* by peroxynitrite appears to be caused by membrane damage. *Microbiology,* 148**,** 307-14.

GERHARDT, P. & MARQUIS, R. E. 1989. Spore thermoresistance mechanisms. *American Society for Microbiology***,** 43-63.

GERHARDT, P., PANKRATZ, H. & SCHERRER, R. 1976. Fine Structure of the *Bacillus thuringiensis* Spore. *Appl Environ Microbiol,* 32.

GRIFFITH, J., MAKHOV, A., SANTIAGOLARA, L. & SETLOW, P. 1994. Electron-Microscopic Studies of the Interaction between a *Bacillus-Subtilis* Alpha/Beta-Type Small, Acid-Soluble Spore Protein with DNA - Protein-Binding Is Cooperative, Stiffens the DNA, and Induces Negative Supercoiling. *Proc Natl Acad Sci U S A,* 91**,** 8224-8228.

HEREMANS, K. & SMELLER, L. 1998. Protein structure and dynamics at high pressure. *Biochim Biophys Acta,* 1386**,** 353-70.

HOFFMAN, R. K., GAMBILL, V. M. & BUCHANAN, L. M. 1968. Effect of cell moisture on the thermal inactivation rate of bacterial spores. *Appl Microbiol,* 16**,** 1240-4.

INGLESBY, T. V., HENDERSON, D. A., BARTLETT, J. G., ASCHER, M. S., EITZEN, E., FRIEDLANDER, A. M., HAUER, J., MCDADE, J., OSTERHOLM, M. T., O'TOOLE, T., PARKER, G., PERL, T. M., RUSSELL, P. K. & TONAT, K. 1999. Anthrax as a biological weapon: medical and public health management. Working Group on Civilian Biodefense. *JAMA,* 281**,** 1735-45.

JUNG, J. H., LEE, J. E., LEE, C. H., KIM, S. S. & LEE, B. U. 2009. Treatment of fungal bioaerosols by a high-temperature, short-time process in a continuous-flow system. *Appl Environ Microbiol,* 75**,** 2742-9.

KAVIANY, M. 1995. *Principles of Heat Transfer in Porous Media*, Springer-Verlag.

KIDA, N., MOCHIZUKI, Y. & TAGUCHI, F. 2004. An effective iodide formulation for killing *Bacillus* and *Geobacillus* spores over a wide temperature range. *J Appl Microbiol,* 97**,** 402-9.

KOURNIKAKIS, B., MARTINEZ, K. F., MCCLEERY, R. E., SHADOMY, S. V. & RAMOS, G. 2011. Anthrax letters in an open office environment: effects of selected CDC response guidelines on personal exposure and building contamination. *J Occup Environ Hyg,* 8**,** 113-22.

LAI, E. M., PHADKE, N. D., KACHMAN, M. T., GIORNO, R., VAZQUEZ, S., VAZQUEZ, J. A., MADDOCK, J. R. & DRIKS, A. 2003. Proteomic analysis of the spore coats of *Bacillus subtilis* and *Bacillus anthracis*. *Journal of Bacteriology,* 185**,** 1443-1454.

LARSON, M. A. & MARINAS, B. J. 2003. Inactivation of *Bacillus subtilis* spores with ozone and monochloramine. *Water Res,* 37**,** 833-44.

LEE, J. H., WU, C. Y., WYSOCKI, K. M., FARRAH, S. & WANDER, J. 2008. Efficacy of iodine-treated biocidal filter media against bacterial spore aerosols. *J Appl Microbiol,* 105**,** 1318-26.

LEE, Y. H. & LEE, B. U. 2006. Inactivation of Airborne E. coli and *B. subtilis* Bioaerosols Utilizing Thermal Energy. *J. Microbiol. Biotechnol,* 16**,** 1684–1689.

MCDONNELL, G. & RUSSELL, A. D. 1999. Antiseptics and disinfectants: Activity, action, and resistance. *Clinical Microbiology Reviews,* 12**,** 147-+.

MCKENNEY, P. T. & EICHENBERGER, P. 2012. Dynamics of spore coat morphogenesis in *Bacillus subtilis*. *Molecular Microbiology,* 83**,** 245-260.

MIYATA, S., KOZUKA, S., YASUDA, Y., CHEN, Y., MORIYAMA, R., TOCHIKUBO, K. & MAKINO, S. 1997. Localization of germination-specific spore-lytic enzymes in Clostridium perfringens S40 spores detected by immunoelectron microscopy. *FEMS Microbiol Lett,* 152**,** 243-7.

MULLICAN, C. L., BUCHANAN, L. M. & HOFFMAN, R. K. 1971. Thermal inactivation of aerosolized *Bacillus subtilis var. niger* spores. *Appl Microbiol,* 22**,** 557-9.

NICHOLSON, W. L., MUNAKATA, N., HORNECK, G., MELOSH, H. J. & SETLOW, P. 2000. Resistance of *Bacillus* endospores to extreme terrestrial and extraterrestrial environments. *Microbiology and Molecular Biology Reviews,* 64**,** 548-+.

PAIDHUNGAT, M., SETLOW, B., DRIKS, A. & SETLOW, P. 2000. Characterization of spores of *Bacillus subtilis* which lack dipicolinic acid. *Journal of Bacteriology,* 182**,** 5505-5512.

PENNELL, K. G., ARONSON, A. I. & BLATCHLEY, E. R., 3RD 2008. Phenotypic persistence and external shielding ultraviolet radiation inactivation kinetic model. *J Appl Microbiol,* 104**,** 1192-202.

REDMOND, C., BAILLIE, L. W. J., HIBBS, S., MOIR, A. J. G. & MOIR, A. 2004. Identification of proteins in the exosporium of *Bacillus anthracis*. *Microbiology-Sgm,* 150**,** 355-363.

RUSSELL, A. D. 1996. Activity of biocides against mycobacteria. *Soc Appl Bacteriol Symp Ser,* 25**,** 87S-101S.

RUSSELL, A. D. 1998. Mechanisms of bacterial resistance to antibiotics and biocides. *Prog Med Chem,* 35**,** 133-97.

SERWAY, R. A. & JEWETT, J. W. 2004. *Physics for Scientists and Engineers*, Cengage Learning.

SETLOW, P. 1995. Mechanisms for the Prevention of Damage to DNA in Spores of *Bacillus* Species. *Annual Review of Microbiology,* 49**,** 29-54.

SETLOW, P. 2003. Spore germination. *Current Opinion in Microbiology,* 6**,** 550-556.

SETLOW, P. 2005. Spores of *Bacillus subtilis*: their reistance to and killing by radiation, heat and chemicals. *J Appl Microbiol*.

TENNEN, R., SETLOW, B., DAVIS, K. L., LOSHON, C. A. & SETLOW, P. 2000. Mechanisms of killing of spores of *Bacillus subtilis* by iodine, glutaraldehyde and nitrous acid. *J Appl Microbiol,* 89**,** 330-8.

TILTON, R. F., JR., DEWAN, J. C. & PETSKO, G. A. 1992. Effects of temperature on protein structure and dynamics: X-ray crystallographic studies of the protein ribonuclease-A at nine different temperatures from 98 to 320 K. *Biochemistry,* 31**,** 2469-81.

TODD, S. J., MOIR, A. J. G., JOHNSON, M. J. & MOIR, A. 2003. Genes of *Bacillus cereus* and *Bacillus anthracis* encoding proteins of the exosporium. *Journal of Bacteriology,* 185**,** 3373-3378.

TOMMASI, E. D., REA, I., RENDINA, I., ROTIROTI, L. & STEFANO, L. D. 2009. Protein conformational changes revealed by optical spectroscopic reflectometry in porous silicon multilayers. *J Phys Condens Matter,* 21**,** 035115.

WATSON, H. E. 1908. A Note on the Variation of the Rate of Disinfection with Change in the Concentration of the Disinfectant. *J Hyg (Lond),* 8**,** 536-42.

ZHANG, P. F., THOMAS, S., LI, Y. Q. & SETLOW, P. 2012. Effects of Cortex Peptidoglycan Structure and Cortex Hydrolysis on the Kinetics of Ca(2+)-Dipicolinic Acid Release during *Bacillus subtilis* Spore Germination. *Journal of Bacteriology,* 194**,** 646-652.

DEPARTMENT OF DEFENSE

DEFENSE THREAT REDUCTION
AGENCY
8725 JOHN J. KINGMAN ROAD
STOP 6201
FORT BELVOIR, VA 22060
ATTN: S. PEIRIS

DEFENSE TECHNICAL
INFORMATION CENTER
8725 JOHN J. KINGMAN ROAD,
SUITE 0944
FT. BELVOIR, VA 22060-6201
ATTN: DTIC/OCA

DEPARTMENT OF DEFENSE CONTRACTORS

QUANTERION SOLUTIONS, INC.
1680 TEXAS STREET, SE
KIRTLAND AFB, NM 87117-5669
ATTN: DTRIAC